

1 Title: **SARS-CoV-2 has observably higher propensity to accept uracil as nucleotide**
2 **substitution: Prevalence of amino acid substitutions and their predicted functional**
3 **implications in circulating SARS-CoV-2 in India up to July, 2020**

4 **Authors:** Subrata Roy¹, Himadri Nath¹, Abinash Mallick¹, Subhajit Biswas^{1*}

5

6 **Affiliations:**

7 *1. Infectious Diseases and Immunology Division, CSIR- Indian Institute of Chemical Biology,*
8 *Kolkata, West Bengal, India.*

9

10 **Address for correspondence**

11 * Dr. Subhajit Biswas, CSIR-Indian Institute of Chemical Biology, 4, Raja S.C. Mullick
12 Road, Kolkata, PIN-700032, West Bengal, India. Email: subhajit.biswas@iicb.res.in;
13 subhajitcam@gmail.com; Phone: (+) 91-(0) 33-2499-5776. Fax: (+) 91-(0) 33-2473-5197;
14 (+) 91-(0) 33-2472-3967.

15

16 **Abstract:**

17 SARS-CoV-2 has emerged as pandemic all over the world since late 2019. In this study, we
18 investigated the diversity of the virus in the context of SARS-CoV-2 spread in India. Full-
19 length SARS-CoV-2 genome sequences of the circulating viruses from all over India were
20 collected from GISAID, an open data repository, until 25th July, 2020. We have focused on
21 the non-synonymous changes across the genome that resulted in amino acid substitutions.
22 Analysis of the genomic signatures of the non-synonymous mutations demonstrated a strong
23 association between the time of sample collection and the accumulation of genetic diversity.
24 Most of these isolates from India belonged to the A2a clade (63.4%) which has overcome the
25 selective pressure and is spreading rapidly across several continents. Interestingly a new
26 clade I/A3i has emerged as the second-highest prevalent type among the Indian isolates,
27 comprising 25.5% of the Indian sequences. Emergence of new mutations in the S protein was
28 observed. Major SARS-CoV-2 clades in India have defining mutations in the RdRp.
29 Maximum accumulation of mutations was observed in ORF1a.

30 Other than the clade-defining mutations, few representative non-synonymous mutations were
31 checked against the available crystal structures of the SARS-CoV-2 proteins in the DynaMut
32 server to assess their thermodynamic stability. We have observed that SARS-CoV-2 genomes
33 contain more uracil than any other nucleotide. Furthermore, substitution of nucleotides to
34 uracil was highest among the non-synonymous mutations observed. The A+U content in
35 SARS-CoV-2 genome is much higher compared to other RNA viruses, suggesting that the
36 virus RdRp has a propensity towards uracil incorporation in the genome. This implies that
37 thymidine analogues may have a better chance to competitively inhibit SARS-CoV-2 RNA
38 replication than other nucleotide analogues.

39 **Keywords:** SARS-CoV-2, uracil, non-synonymous mutation

40 **1. Introduction:**

41 The world is in a pandemic situation due to an outbreak of highly infectious human to human
42 transmissible virus, named SARS-CoV-2. Since the first novel pneumonia case in Wuhan,
43 China 17,396,943 confirmed cases with 675,060 deaths were reported until 1st August 2020
44 (WHO, 2020). The virus was found to be a strain of beta-coronavirus and related to SARS-
45 like BAT coronaviruses, bat-SL-CoVZC45 and bat-SL-CoVZXC21 with 88% similarity;
46 79.5% homology with SARS, and 50% with MERS (Lu *et al.*, 2020; Wu *et al.*, 2020). The
47 virus originated from its root (Wuhan) and is changing while spreading throughout the world.
48 It is an RNA virus with a higher mutation rate over DNA viruses. Therefore, characterisation
49 of circulating strains is important to correlate with disease pathogenesis and outcome; decide
50 on treatment strategies as well as to obtain real-time background information for developing
51 effective vaccines and antivirals.

52 Over the few months, several studies have been published which reported some novel
53 mutations in Indian isolates. In this study, whole-genome mutation analysis has been done for
54 a total of 1878 sequences that have been reported from India. Nucleotide changes that have
55 introduced non-synonymous changes in the gene have been considered for analysis. Here, all
56 the sequences were analyzed to find in which clades they fit best in respect to the global
57 scenario. In this study, we have presented a clear understanding of the mutations prevalent in
58 SARS-CoV-2 isolates from India till the end of July 2020.

59

60 **2. Materials and methods:**

61 Since the outbreak of SARS-CoV-2 in China in December 2019, GISAID
62 (<https://www.gisaid.org/>) has become a global repository for coronavirus genome sequences.
63 For this study, 365 full genome sequences from India until 25th May, 2020 were collected

64 from the GISAID server. Later 1513 more sequences were added to this study to compare
65 the pattern of SARS-CoV-2 spread across India. Sequences were aligned using the MEGA X
66 software (Kumar *et al.*, 2018). Position of amino acids was defined with respect of the first
67 viral genome sequence, named nCoV2019-Wuhan-hu-1/2019 (GenBank accession no:
68 MN908947), taken as the parental or reference strain in the multiple sequence alignment.
69 Analysis of data was done using Bioedit (Hall, Biosciences and Carlsbad, 2011).

70 The functional implications of non-synonymous mutations were predicted in the DynaMut
71 (Rodrigues *et al.*, 2018) server utilizing the available crystal structure data specific to SARS-
72 CoV-2 proteins. Several mutations which were found to be selective in the population;
73 reported previously as important, or used as a marker to define different clades, were studied
74 in DynaMut to study their functional importance. DynaMut score $\Delta\Delta G$ for each mutation was
75 considered to predict whether the mutation is stabilizing or not. In order to predict the
76 flexibility of a protein with a given mutation, the free entropy change was considered and this
77 also gives the prediction of future selectivity of the said mutation. Flexibility and rigidity are
78 the key contributors to protein function. Consequently, in higher temperature fluctuations, a
79 rigid protein structure is beneficial for protein structure stability rather than a flexible
80 structure (M, 1987). In our DynaMut studies, $\Delta\Delta S_{Vib} ENCoM$ is the change in vibrational
81 entropy energy between wild-type and mutant protein. The value of $\Delta\Delta S_{Vib} ENCoM$
82 predicted in the DynaMut server for each point mutation signifies the change in the molecular
83 flexibility of the protein. Negative value indicates a decrease in flexibility and vice versa.
84 This means mutations that confer potential structural rigidity to the proteins ($\Delta\Delta G$ value
85 positive; $\Delta\Delta S_{Vib} ENCoM$, negative) might compensate for higher temperature oscillations.
86 Hence based on the calculative predictions, such mutations may constitute a stable
87 conformation of the proteins in the virus evolution.

88 In this study, the potential impact of a point mutation in the protein structure was also
89 predicted via free energy-based (ΔG) calculative method in DynaMut server. Low free energy
90 value signifies a stable protein conformation and high free energy value for unstable protein
91 conformation. So, if an amino acid substitution lowers the free energy value from the wild
92 type, the mutation dictates a stabilizing conformation of the protein. From the DynaMut
93 server, we obtained a $\Delta\Delta G$ value which means a difference between ΔG wildtype and ΔG
94 mutation ($\Delta\Delta G = \Delta G$ wildtype - ΔG mutation).

95

96 **3. Results:**

97 **3.1. Defining types of SARS-CoV-2**

98 Overall, a high level of sequence identity throughout the 29 kb genome was observed
99 considering the single nucleotide polymorphisms that resulted in change of amino acids in
100 comparison to the reference sequence (MN908947.3). Other than the clade-defining ones,
101 mutations that occurred on more than ten occasions (considering all sequences), have been
102 used in our analysis. Others have been ignored as they may be sequencing artefacts.
103 According to previous reports, the earliest sequences of SARS-CoV-2 from China belonged
104 to clade O. In addition to the ancestral type (O), there were 10 derived types. Among them
105 five derived types had high frequencies in India, namely O, B, B1, A1a, and A2a up to early
106 May, 2020 (Biswas and Majumder, 2020).

107 In total, 1190 isolates contained both D614G (nt 23403 A>G) in spike protein along with
108 P323L (nt 14408C>T) in RdRp of ORF1b which group them under the A2a clade. The
109 viruses of clade A2a constituted 63.4% of the total reported sequences in India. Twenty-
110 seven isolates were A3 type (1.4%), containing the clade-defining mutations V378I (nt
111 1397G>A) and L3606F (nt 11083G>T) in ORF1a. Total 82 isolates from India contained

112 L84S (nt 28144T>C) mutation in ORF8 which is a clade-defining mutation for B type.
113 Among them, 73 isolates also had S202N (nt 28878G>A) mutation in N gene as well. These
114 73 isolates belonged to B4 type (3.9%). Among the rest 9 isolates, 8 isolates were of B type
115 (0.4%) (Fig: 1). Therefore, it appears that B4 emerged from B and predominated among the B
116 types over the duration of our study. The other isolate with the L84S mutation belonged to
117 A2a type (Supplementary Table 1).

118 Up to 1st May, 2020 only 8 out of the total 56 Indian isolates reported till that time, contained
119 some novel mutations i.e. P13L (nt 28311C>T, N gene), A97V (nt 13730C>T in RdRp
120 ORF1b) and T2016K (nt 6312C>A) along with L3606F (nt 11083G>T) in ORF1a. Later,
121 with more and more sequences being available, a different cluster gradually emerged with the
122 above three clade-defining mutations. This clade had been named I/A3i (Jolly *et al.*, 2020).
123 In case of few isolates, any one of the above-mentioned mutations could not be determined
124 but rest were present, so those genomes had been included within the I/A3i type.
125 Interestingly, this cluster was found to constitute 40% of the total reported sequences in India
126 until 25th May. However, the scenario changed on extending our study to the end of July. The
127 I/A3i type decreased to 25.5% of the total sequence observed, while A2a subtype increased
128 from 50% to 63% of the total study population. Emergence of another subtype was observed
129 in the form of A2 in case of the SARS-CoV-2-infected Indian population. Until the end of
130 May, no A2 subtype was observed which carried only the D614G mutation in the spike
131 protein. But extended study identified 61 sequences (3.2%) of A2 subtype in the Indian
132 population. In case of 31 Indian isolates, specific clade couldn't be assigned due to lack of
133 sufficient or confirmed sequence information in the clade-defining positions.

134

135

136 **3.2.Other non-synonymous mutations:**

137 Our study has identified some other mutations among the different clades which may play an
138 important role in the course of viral genome divergence (Table 1). For instance, besides the
139 clade-defining mutations, two other mutations were observed in high frequency (n=20/27
140 each) in the A3 cluster; i.e. R207C and M2796I in nsp2 and nsp4 respectively.

141 Two consecutive amino acid changes R203K and G204R could be observed in the
142 nucleocapsid phosphoprotein (N protein) of approx. 30% A2 and 37% A2a Indian isolates.
143 These mutations were previously reported to be also abundant in the USA (Joshi and Paul,
144 2020). Over the course of infection A2a type has acquired highest number of mutations in
145 ORF1a such as, S318L (n=34/1190) and Q676P (n=55/1190) in nsp2; A1812D (n=232/1190)
146 and S2103F (n=112/1190) in nsp3; D3042N (n=34/1190) and A3143V (n=69/1190) in nsp4
147 and S3517F (n=38/1190) in nsp5 of ORF1a (Fig:2). Similarly, A2a type also showed non-
148 synonymous changes in other regions, like Q57H (n=328/1190) and L46F (n=109/1190) in
149 ORF3a and S194L (n=187/1190) in the N gene. Another mutation in N gene P13L was
150 observed abundantly in I/A3i type (n=412/478). Other mutations in ORF1a, like G519S
151 (n=34/478) and S2015R (n=61/478) were observed with a high frequency of occurrence in
152 I/A3i clade. The newly emerged A2 type in India also showed high number of mutations in
153 ORF1a as observed in case of the A2a type (details in Table 1).

154

155 **3.3.DynaMut Analysis**

156 DynaMut analysis was done to predict the effect of a point mutation on respective protein
157 stability and molecular flexibility. In the case of spike protein, the mutation D614G had a
158 structurally stabilizing effect on the protein in terms of free energy change ($\Delta\Delta G$) (Table 2)
159 and is a clade-defining stable mutation for A2 and A2a types. Similarly in case of nsp12
160 (RdRp), two clade-defining mutations A97V and P323L also appeared to have stabilizing
161 effect on the RNA polymerase, with decreased molecular flexibility (Karshikoff, Nilsson and
162 Ladenstein, 2015). A representative mutation in nsp3 i.e. I1159M was found to be
163 destabilizing and occurred at lower frequency(n=14). Interestingly, DynaMut analysis
164 revealed R408I mutation in S protein to be a stabilizing one but this mutation appeared on a
165 single occasion in a O type virus among all sequences analyzed (Table 2).

166

167 **3.4.The propensity of the nucleotide changes**

168 The SARS-CoV-2 viral genome is made up of 62% A+U content while the G+C content is
169 38%. In our study, we have observed that uracil content (32% of the total genome) was much
170 higher in SARS-CoV-2 compared to other RNA viruses like Dengue (20%) or Chikungunya
171 (20%) (Fig: 3). Furthermore, it was found that majority of the non-synonymous mutations
172 occurred due to change of other nucleotides to uracil (64% of the total non-synonymous
173 mutations analysed). The highest rate of substitution was observed as cytosine to uracil (40%
174 of the total number of mutations). (Fig: 4)

175

176 **4. Discussion:**

177 Since the outbreak of the SARS-CoV-2, it spread rapidly to more than 200 countries in
178 different continents. Notably, the USA and Western European countries like Spain and Italy
179 had seen a high rate of mortality. Until August 1st, 2020 India has reported 1,695,988
180 confirmed cases and 36,511 deaths due to COVID-19 (WHO, 2020). Compared to the global
181 scenario where death rate due to SARS-CoV-2 was 3.8%, a densely populated country like
182 India had reported only 2.15% mortality due to this highly transmissible virus.

183 This study was done to understand whether the observed geographical variations in the
184 prevalence of infection, had any relation with particular SARS-CoV-2 clusters. The study
185 was done to assess pathogen evolution with disease transmission. Studies have revealed that a
186 particular subtype A2a, had spread rapidly throughout the European and North American
187 continents and entered East Asia in January 2020. The spread of this subtype rapidly
188 increased from 2% to 60% within 10 weeks (Bhattacharyya *et al.*, 2020).

189 Most of the sequences from India belonged to the A2a subtype before 1st May. But another
190 cluster of sequences was reported later and classified as I/A3i subtype (Jolly *et al.*, 2020).
191 Surprisingly, the spread of the I/A3i subtype escalated from 14% to 40% of the total reported
192 sequence within 3 weeks (1st May to 25th May 2020). Later the spread of I/A3i decreased to
193 25.5% of the total infections by the end of July. Over this time, the A2 type (3%) of SARS-
194 CoV-2 emerged in the Indian population, which contained only D614G mutation in the spike
195 protein as the clade-defining mutation. In the time period covered, mainly two types of
196 SARS-CoV-2 isolates were prevalent in India i.e. A2a (63.4%) and I/A3i (25.5%). Other
197 isolates mainly belonged to B4 (3.9%), A3 (1.4%), B (0.4%), O (0.3%) and A1a (0.2%) types
198 (Fig 1).

199 The most-mentioned mutation in the spike protein, D614G, was observed in all the Indian A2
200 and A2a sequences (1256 out of 1878 genomes). It has been suggested as one of the major
201 factors behind the virulence of the virus (Korber *et al.*, 2020). However, the position of this
202 mutation is far away from the RBD. Reports suggested that D614G mutation at the junction
203 of the S1 and S2 subunits of S gene introduces an additional cleavage site in the S protein
204 (Bhattacharyya *et al.*, 2020). It has been predicted to reduce host immune response by
205 producing “decoy” fragments that bind to and inactivate antiviral antibodies (Park *et al.*,
206 2016). This was anticipated to help the virus evade the primary immune response and
207 establish an infection rapidly. It had been experimentally shown that D614G mutation can
208 also increase infectivity substantially by facilitating receptor-ligand interactions (Zhang *et al.*,
209 2020). Two other notable mutations P323L in RdRp and C241T (synonymous nucleotide
210 change) in 5' UTR are co-evolving with this mutation. Coronaviruses contain sub-genomic
211 identical 5' leader sequence which plays a role in virus replication. It will be interesting to see
212 whether these changes have any influence on altering the efficiency of viral replication or
213 not.

214 Two highly predominant clades I/A3i and A2a in India contain distinct mutations in nsp12,
215 i.e. A97V and P323L respectively. These non-synonymous mutations have been used to
216 define clade as well. So, the virus is possibly adapting through gain of mutations in the RdRp
217 and possibly towards more effective replication potential. This proposition also needs
218 experimental validation.

219 In our analysis, 31 isolates could not be assigned to any specific clade as they either
220 contained mutations overlapping different clades or ‘N’/s (i.e. nucleotide/s could not be
221 determined by sequencing) at clade-defining areas of the genomes. One such isolate from
222 Gujrat (hCoV-19/India/GBRC24b/2020|EPI_ISL_437454|2020-04-26) showed a unique
223 combination of mutations from two different types. This isolate contains P323L (nt

224 14408C>T) in nsp12 but not D614G (nt 23403A>G) in the S gene which is required to define
225 it as an A2a type. On the other hand, this also contains T2016K (nt 6312C>A) in nsp3 and
226 A97V (nt 13730C>T) in nsp12 but does not have L3606F (nt 11083G>T) in nsp6. So, it
227 could not be established as a genuine I/A3i type also. It appears to be either a
228 hybrid/recombinant of the two types. Alternatively, the patient might have been infected with
229 two different types of SARS-CoV-2 and this peculiar genome sequence is the artefact of
230 sequence assembly of reads generated from mixed sequences.

231 As the prevalence of A2a and I/A3i is increasing rapidly, we need to observe closely for these
232 kinds of isolates. It has been observed that of P13L (nt C28311T) and S194L (nt C28863T)
233 mutations in nucleocapsid protein are emerging at high frequency among recently uploaded
234 sequences from India. For instance, the distribution of the P13L mutation in I/A3i clade
235 (n=412 out of 478) suggests that it is perhaps evolving towards becoming a clade-defining
236 mutation for I/A3i. S194L mutation was only observed among A2a and A2 types of the
237 Indian isolates.

238 Non-synonymous mutations that were encountered on ≥ 10 occasions were considered in our
239 study. DynaMut analysis was performed for those SARS-CoV-2 proteins for which the
240 crystal structure data were available. Mutations such as D614G in S protein and A97V and
241 P323L in nsp12 were found to be stabilizing by the DynaMut analysis. Their predicted
242 stability was further supported by the observed high frequency of these mutations suggesting
243 that these mutations are getting fixed in the population. Interestingly, the R408I mutation (nt
244 G22785T, n=1) in S protein was predicted as a stable mutation by the DynaMut programme
245 and had been previously reported as a potential RBD-altering mutation (Saha *et al.*, 2020).
246 However, this mutation did not appear to have any significance in the selection of the viral
247 genomes. Since its reporting, this mutation in the O type backbone was never encountered
248 anymore in the sequences that became predominant henceforth, namely A2a and I/A3i.

249 Instead, the S protein had acquired another mutation, L54F at a high frequency among A2a
250 and A2 types where D614G is predominant. DynaMut analysis of L54F mutation has also
251 identified it as a stabilizing one.

252 A2a subtype had acquired the greatest number of mutations in ORF1a compared to other
253 subtypes. Among them S318L (nt C1218T) and Q676P (nt A2292C) in nsp2; S1515F (nt
254 C4809T), I1159M (nt A3742G), S1534I (C4809T), A1812D (nt C5700A) and S2013F (nt
255 C6573T) in nsp3; D3042N (nt G9389A) and A3143V (nt C9693T) in nsp4, S3517F (nt
256 C10815T) in nsp5 and L3606F (nt G11083T) in nsp6 were highly frequent in the population.
257 Three mutations in N gene S194L (nt C28854T), R203K (nt G28881A) and G204R (nt
258 G28883C) were also found to be abundant within the A2a subtype. Furthermore, some
259 researches indicated that a part of the nucleocapsid (N) protein of SARS-CoV (aa 161–211) is
260 required for interacting with human cellular heterogeneous nuclear ribonucleoprotein A1 and
261 this can play a regulatory role in the synthesis of SARS-CoV RNAs (Luo *et al.*, 2005). So, it
262 would be interesting to see whether these mutations affect SARS-CoV-2 replication or not.

263 Other mutations like L46F (nt C25528T) and Q57H (nt G25563T) in ORF3a were observed
264 among the A2a isolates at high frequency. The 3a protein was predicted to be a
265 transmembrane protein (Zeng *et al.*, 2004) and may be involved in ion channel formation
266 during infection by co-localizing in the Golgi network (Lu, Xu and Sun, 2010). However, the
267 Q57H mutation does not occur in the 6 defined domains of ORF3a (Issa *et al.*, 2020). It will
268 be interesting to investigate whether these mutations have any role in virus transmission or
269 replication.

270 From the perspective of the Indian isolates, occurrence of mutations in ORF1a was observed
271 at higher number. Among the non-structural proteins of ORF1a, nsp3 (papain-like protease)
272 tends to accumulate the highest number of mutations. When overall frequencies were

273 compared, D614G in S protein and P323L in nsp12 were found to be highest along with a
274 synonymous nucleotide change C241T in 5'UTR among all the Indian sequences (Fig 2).

275 SARS-CoV-2 genome is made up of 29.94% adenine, 18.37% guanine, 19.61% cytosine and
276 32.08% uracil. Compared to other RNA viruses (i.e. Dengue, Chikungunya) SARS-CoV-2
277 contains a higher amount of uracil (Fig 3). Interestingly, the most frequent changes in
278 nucleotide were observed as C>T in case of non-synonymous mutations (Fig 4). This virus
279 tends to change nucleotides into uracil at a high frequency which indicates the biasness of
280 viral RdRp. These findings can help in selecting effective nucleoside/nucleotide analogues to
281 test as effective antivirals. Analogously, herpes simplex virus (HSV) genome is GC-rich and
282 9-(2-hydroxyethoxymethyl) guanine (Acyclovir), the “gold-standard” herpes antiviral is
283 incidentally a guanosine analogue. Acyclovir was the first highly virus-selective antiviral
284 drug. It serves as a more preferential substrate for the HSV-encoded thymidine-kinase than
285 host cell kinases for its initial phosphorylation (Frobert *et al.*, 2005; Jiao *et al.*, 2019).
286 Previously, 3'-azido-2',3'-unsaturated thymine analogue has shown better activity compared
287 to other nucleoside analogues against SARS-CoV (EC₅₀=10.3 μM) with a significant level of
288 toxicity (Chu *et al.*, 2006). These findings will be helpful towards developing new antiviral
289 candidates for SARS-CoV-2 where uracil/thymidine analogues may have an upper hand.

290 In summary, the identification and characterization of mutations in the SARS-CoV-2 genome
291 will provide a better understanding of viral genome divergence and disease spread (Fig 5).
292 The observations reported in this study require further experimental confirmation/validation.

293

294

295 **Credit authorship contribution statement:**

296 **Subrata Roy**- Sequence analysis, draft writing, visual representation

297 **Himadri Nath & Abinash Mallick**- DynaMut analysis, review and editing draft.

298 **Subhajit Biswas**- Conceptualization, Supervision and monitoring, Critical review and
299 editing.

300

301 **Acknowledgement:** SR acknowledges UGC for his Senior Research Fellowship. HN & AM
302 thank CSIR for their SRF and JRF respectively. The authors acknowledge CSIR-IICB for
303 providing laboratory facilities for conducting the present work.

304

305 **Funding:** The project was funded by a grant from the **Council of Scientific and Industrial**
306 **Research, India** to S.B. Grant number: MLP 130; CSIR Digital Surveillance Vertical for
307 COVID-19 mitigation in India.

308

309 **Disclosure statement**

310 The authors declare no competing interests.

311

312

313 **Supplementary data:**

314 **Supplementary Table 1. Indian SARS CoV 2 sequences and list of mutations**

315 **References:**

- 316 Bhattacharyya, C. *et al.* (2020) ‘Global Spread of SARS-CoV-2 Subtype with Spike Protein
317 Mutation D614G is Shaped by Human Genomic Variations that Regulate Expression of
318 TMPRSS2 and MX1 Genes’, *bioRxiv*, p. 2020.05.04.075911. doi:
319 10.1101/2020.05.04.075911.
- 320 Biswas, N. and Majumder, P. (2020) ‘Analysis of RNA sequences of 3636 SARS-CoV-2
321 collected from 55 countries reveals selective sweep of one virus type’, *Indian Journal of*
322 *Medical Research*, 0(0), p. 0. doi: 10.4103/ijmr.ijmr_1125_20.
- 323 Chu, C. K. *et al.* (2006) ‘Antiviral activity of nucleoside analogues against SARS-
324 coronavirus (SARS-CoV)’, *Antiviral Chemistry and Chemotherapy*, 17(5), pp. 285–289. doi:
325 10.1177/095632020601700506.
- 326 Frobert, E. *et al.* (2005) ‘Herpes simplex virus thymidine kinase mutations associated with
327 resistance to acyclovir: A site-directed mutagenesis study’, *Antimicrobial Agents and*
328 *Chemotherapy*, 49(3), pp. 1055–1059. doi: 10.1128/AAC.49.3.1055-1059.2005.
- 329 Hall, T., Biosciences, I. and Carlsbad, C. (2011) ‘BioEdit: An important software for
330 molecular biology’, *GERF Bulletin of Biosciences*, 2(June), pp. 60–61. doi:
331 10.1002/prot.24632.
- 332 Issa, E. *et al.* (2020) ‘SARS-CoV-2 and ORF3a: Nonsynonymous Mutations, Functional
333 Domains, and Viral Pathogenesis’, *mSystems*, 5(3), pp. 1–7. doi: 10.1128/msystems.00266-
334 20.
- 335 Jiao, X. *et al.* (2019) ‘Complete Genome Sequence of Herpes Simplex Virus 1 Strain
336 McKrae’, *Microbiology Resource Announcements*, 8(39). doi: 10.1128/mra.00993-19.
- 337 Jolly, B. *et al.* (2020) ‘A distinct phylogenetic cluster of Indian SARS-CoV-2 isolates’, pp.

- 338 1–15.
- 339 Joshi, A. and Paul, S. (2020) ‘Phylogenetic Analysis of the Novel Coronavirus Reveals
340 Important Variants in Indian Strains’, pp. 1–12.
- 341 Karshikoff, A., Nilsson, L. and Ladenstein, R. (2015) ‘Rigidity versus flexibility: The
342 dilemma of understanding protein thermal stability’, *FEBS Journal*. Blackwell Publishing
343 Ltd, pp. 3899–3917. doi: 10.1111/febs.13343.
- 344 Korber, B. *et al.* (2020) ‘Spike mutation pipeline reveals the emergence of a more
345 transmissible form of SARS-CoV-2’, *bioRxiv*, p. 2020.04.29.069054. doi:
346 10.1101/2020.04.29.069054.
- 347 Kumar, S. *et al.* (2018) ‘MEGA X: Molecular evolutionary genetics analysis across
348 computing platforms’, *Molecular Biology and Evolution*, 35(6), pp. 1547–1549. doi:
349 10.1093/molbev/msy096.
- 350 Lu, R. *et al.* (2020) ‘Genomic characterisation and epidemiology of 2019 novel coronavirus:
351 implications for virus origins and receptor binding’, *The Lancet*, 395(10224), pp. 565–574.
352 doi: 10.1016/S0140-6736(20)30251-8.
- 353 Lu, W., Xu, K. and Sun, B. (2010) ‘SARS accessory proteins ORF3a and 9b and their
354 functional analysis’, in *Molecular Biology of the SARS-Coronavirus*. Springer Berlin
355 Heidelberg, pp. 167–175. doi: 10.1007/978-3-642-03683-5_11.
- 356 Luo, H. *et al.* (2005) ‘The nucleocapsid protein of SARS coronavirus has a high binding
357 affinity to the human cellular heterogeneous nuclear ribonucleoprotein A1’, *FEBS Letters*,
358 579(12), pp. 2623–2628. doi: 10.1016/j.febslet.2005.03.080.
- 359 M, V. (1987) ‘Relationship of protein flexibility to thermostability.’, *Protein Engineering*,
360 1(6), pp. 477–480. doi: 10.1093/PROTEIN/1.6.477.

- 361 Park, J. E. *et al.* (2016) ‘Proteolytic processing of middle east respiratory syndrome
362 coronavirus spikes expands virus tropism’, *Proceedings of the National Academy of Sciences
363 of the United States of America*, 113(43), pp. 12262–12267. doi: 10.1073/pnas.1608147113.
- 364 Rodrigues, C. H. *et al.* (2018) ‘DynaMut: predicting the impact of mutations on protein
365 conformation, flexibility and stability’, *Nucleic Acids Research*, 46. doi: 10.1093/nar/gky300.
- 366 Saha, P. *et al.* (2020) ‘A virus that has gone viral: Amino acid mutation in S protein of Indian
367 isolate of Coronavirus COVID-19 might impact receptor binding and thus infectivity’,
368 *bioRxiv*, p. 2020.04.07.029132. doi: 10.1101/2020.04.07.029132.
- 369 WHO (2020) *Coronavirus disease (COVID-19) Situation Report-194*.
- 370 Wu, F. *et al.* (2020) ‘A new coronavirus associated with human respiratory disease in China’,
371 *Nature*, 579(7798), pp. 265–269. doi: 10.1038/s41586-020-2008-3.
- 372 Zeng, R. *et al.* (2004) ‘Characterization of the 3a protein of SARS-associated coronavirus in
373 infected vero E6 cells and SARS patients’, *Journal of Molecular Biology*, 341(1), pp. 271–
374 279. doi: 10.1016/j.jmb.2004.06.016.
- 375 Zhang, L. *et al.* (2020) ‘The D614G mutation in the SARS-CoV-2 spike protein reduces S1
376 shedding and increases infectivity.’, *bioRxiv*: *the preprint server for biology*, p.
377 2020.06.12.148726. doi: 10.1101/2020.06.12.148726.
- 378
- 379

Type	Gene	Defining mutation(s) for individual clades	Other mutations	Nucleotide position	Gene	Frequency of other mutations*	
O (n=6)	S		R408I	G22785T		1	
B (n=8)	ORF1a		V2586G	T8022G	nsp3	1	
	ORF8	L84S (nt: T28144C)					
	N gene		P13L	C28311T		1	
B4 (n=73)	ORF1a		Q676P	A2292C	nsp2	4	
			V2586G	T8022G	nsp3	3	
			L3606F	G11083T	nsp6	6	
	ORF1b		L1701F	C18568T	nsp14	4	
			K2566R	A21137G	nsp14	2	
	ORF8	L84S (nt: T28144C)					
	S gene		L54F	G21724T		2	
			D614G	A23403G		4	
	ORF3a		Q57H	G25563T		2	
N	S202N (nt: G28878A)						
A1a (n=4)	ORF1a	L3606F (nt: G11083T) nsp6	V2528G	T8022G	nsp4	1	
	ORF3a	G251V (nt: G26144T)					
A3 (n=27)	ORF1a	V378I (nt: G1397A) nsp2	R207C	C884T	nsp2	20	
			L3606F (nt: G11083T) nsp6	V2528G	T8022G	nsp3	2
				M2796I	G8653T	nsp4	20
A2a (n=1190)	ORF1a		S318L	C1218T	nsp2	34	
			G519S	G1820A	nsp2	5	
			V561F	G1946T	nsp2	6	
			Q676P	A2292C	nsp2	55	
			I1159M	A3742G	nsp3	13	
			S1515F	C4809T	nsp3	20	

			S1534I	G4866T	nsp3	10	
			A1812D	C5700A	nsp3	232	
			S2103F	C6573T	nsp3	112	
			P2376L	C7392T	nsp3	12	
			V2586G	T8022G	nsp3	6	
			D3042N	G9389A	nsp4	34	
			T3058I	C9438T	nsp4	7	
			A3143V	C9693T	nsp4	69	
			S3517F	C10815T	nsp5	38	
			L3606F	G11083T	nsp6	16	
	ORF1b	P323L (nt:C14408T) nsp12	A97V	C13730T	nsp12	7	
			A1169T	G16945A	nsp13	13	
			L1701F	C18568T	nsp14	54	
			K2566R	A21137G	nsp16	4	
	S	D614G (nt: A23403G)	L54F	G21724T		69	
	ORF 8		L84S	T28144C		1	
	ORF3a		L46F	C25528T		109	
			Q57H	G25563T		328	
	N		P13L	C28854T		2	
			S194L	C28311T		187	
			R203K	G28881A		450	
			G204R	G28883C		452	
I/A3i (n=478)	ORF1a	T2016K (nt:C6312A) nsp3	A339V	C1281T	nsp2	14	
			S481F	C1707T	nsp2	11	
			G519S	G1820A	nsp2	34	
			D1939G	A6081G	nsp3	16	
		L3606F (nt: G11083T) nsp6		S2015R	C6310A	nsp3	61
	P2376L			C7392T	nsp3	6	
	V2586G			T8022G	nsp3	18	
	T3058I			C9438T	nsp4	1	
				S3517F	C10815T	nsp5	1
	ORF1b	A97V (nt: C13730T) nsp12		P323L	C14408T	nsp12	5
				K2566R	A21137G	nsp16	4
	S			L54F			1
	N			P13L	C28311T		412
				R203K	G28881A		2
G204R				G28883C		2	

380

A2 (n=61)	ORF1a		Q676P	A2292C	nsp3	16
			A1812D	C5700A	nsp3	9
			S2103F	C6573T	nsp3	2
			D3042N	G9389A	nsp4	1
	ORF1b		A1169T	G16945A	nsp13	1
			L1701F	C18568T	nsp14	14
	S	D614G (nt: A23403G)	L54F	G21724T		14
	ORF3a		Q57H	G25563T		21
			L46F	C25528T		1
	N		S194L	C28311T		27
			S202N	G28878A		2
			R203K	G28881A		18
			G204R	G28883C		17

381

382

383 **Table 1: Non-synonymous mutations and corresponding frequencies across the different**
 384 **clades of Indian SARS-CoV-2 isolates.**

385 *Except the R408I mutation (n=1) in O type S protein, non-synonymous mutations with
 386 cumulative frequency of ≥ 10 , have only been considered.

387

	Mutation	DynaMut $\Delta\Delta G$ (kcal/mol)	$\Delta\Delta S_{Vib} ENCoM$ (Δ Vibrational Entropy Energy between Wild-type and Mutant) (kcal.mol ⁻¹ . K ⁻¹)
S gene (PDB ID: 6VSB)	L54F (n=87)*	1.746 (Stabilizing)	-4.764 (Decrease of molecule flexibility)
	R408I (n=1)	1.857 (Stabilizing)	-4.408 (Decrease of molecule flexibility)
	D614G (n=1256)	1.128 (Stabilizing)	-4.531 (Decrease of molecule flexibility)
ORF 1a	I1159M nsp3 (PDB ID: 6WEY) (n=14)	-0.258 (Destabilizing)	0.309 (Increase of molecule flexibility)
	S3517F nsp5 (PDB ID: 6Y84) (n=39)	1.041 (Stabilizing)	-0.249 (Decrease of molecule flexibility)
ORF1b	A97V nsp12 (PDB ID: 6M71) (n=462)	1.397 (Stabilizing)	-5.146 (Decrease of molecule flexibility)
	P323L nsp12 (PDB ID: 6M71) (n=1210)	1.540 (Stabilizing)	-4.820 kcal.mol ⁻¹ . K ⁻¹ (Decrease of molecule flexibility)

388

389 **Table 2:** Analysis of the mutations and their stability by DynaMut.

390 *Frequency of each mutation was calculated including the 31 Indian sequences which were

391 undefined and could not be assigned to any particular clade.

392 **Figure legends:**

393 **Fig 1: Distribution of different types of SARS-CoV-2 among the Indian population. (a)**

394 Most of the isolates belong to 2 major types of virus, A2a and I/A3i. A new cluster of viruses
395 I/A3i was found to be getting fixed in the population until 25th May 2020. **(b)** The extended
396 study revealed that the percentage of I/A3i decreased from 40% to 25% by 25th July 2020 and
397 A2a became the predominant type.

398

399 **Fig 2: Distribution of non-synonymous mutations across the Indian SARS-CoV-2**

400 **genomes.** Highest accumulation of mutation can be observed in ORF1a compared to the
401 overall genome. Among the non-structural proteins, nsp3 tends to accumulate the greatest
402 number of mutations.

403

404 **Fig 3: Comparison of nucleotide composition of SARS-CoV-2 RNA backbone with that**

405 **of two other prevalent RNA viruses in India.** The frequency of uracil is highest among all
406 four nucleotides in SARS-CoV-2 genomes. This holds true for both older and recently
407 emergent types of SARS-CoV-2 Indian sequences. Average nucleotide distribution in the
408 RNA backbone of each virus was calculated from three sequences for each virus. Error bars
409 represent SD among the three sequences of each virus used in the comparison.

410

411 **Fig 4: Frequency of non-synonymous nucleotide substitutions expressed as a percentage**

412 **of the mutations resulting in amino acid substitutions.** Most frequent changes in
413 nucleotides were observed in form of C>T (40%). Substitution of G to T was recorded

414 second-highest, sharing 20% of the total non-synonymous mutations. Overall, 64% of all the
415 non-synonymous mutations were substitutions to uracil/thymidine.

416

417 **Fig 5: Schematic representation of SARS-CoV-2 types prevalent in the Indian**
418 **population up to July 2020.** It is based on the simplified understanding of the non-
419 synonymous changes that shaped the emergence, divergence and prevalence of the different
420 SARS-CoV-2 types.

421

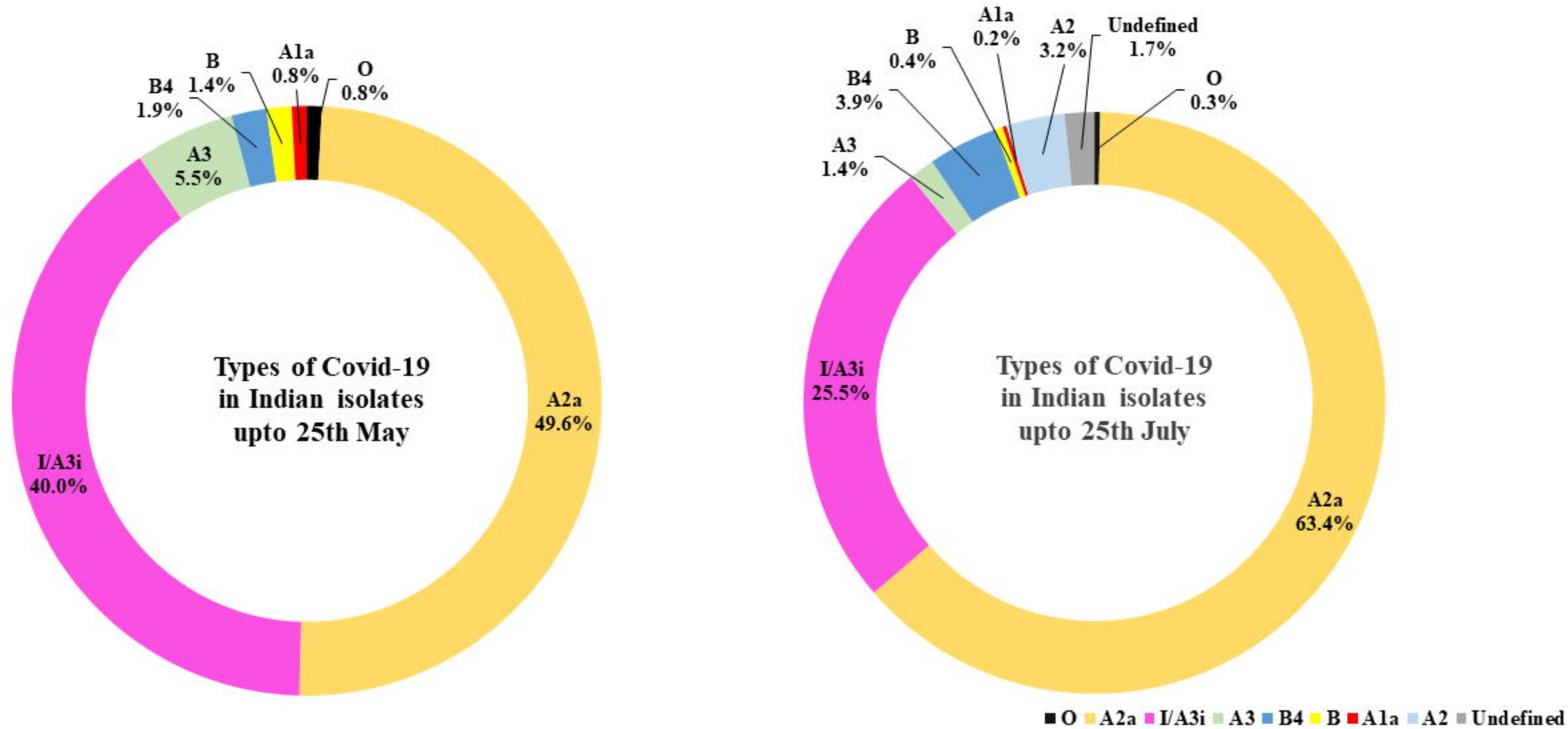


Fig 1: Distribution of different types of SARS-CoV-2 among the Indian population. (a) Most of the isolates belong to 2 major types of virus, A2a and I/A3i. A new cluster of viruses I/A3i was found to be getting fixed in the population until 25th May 2020. (b) The extended study revealed that the percentage of I/A3i decreased from 40% to 25% by 25th July 2020 and A2a became the predominant type.

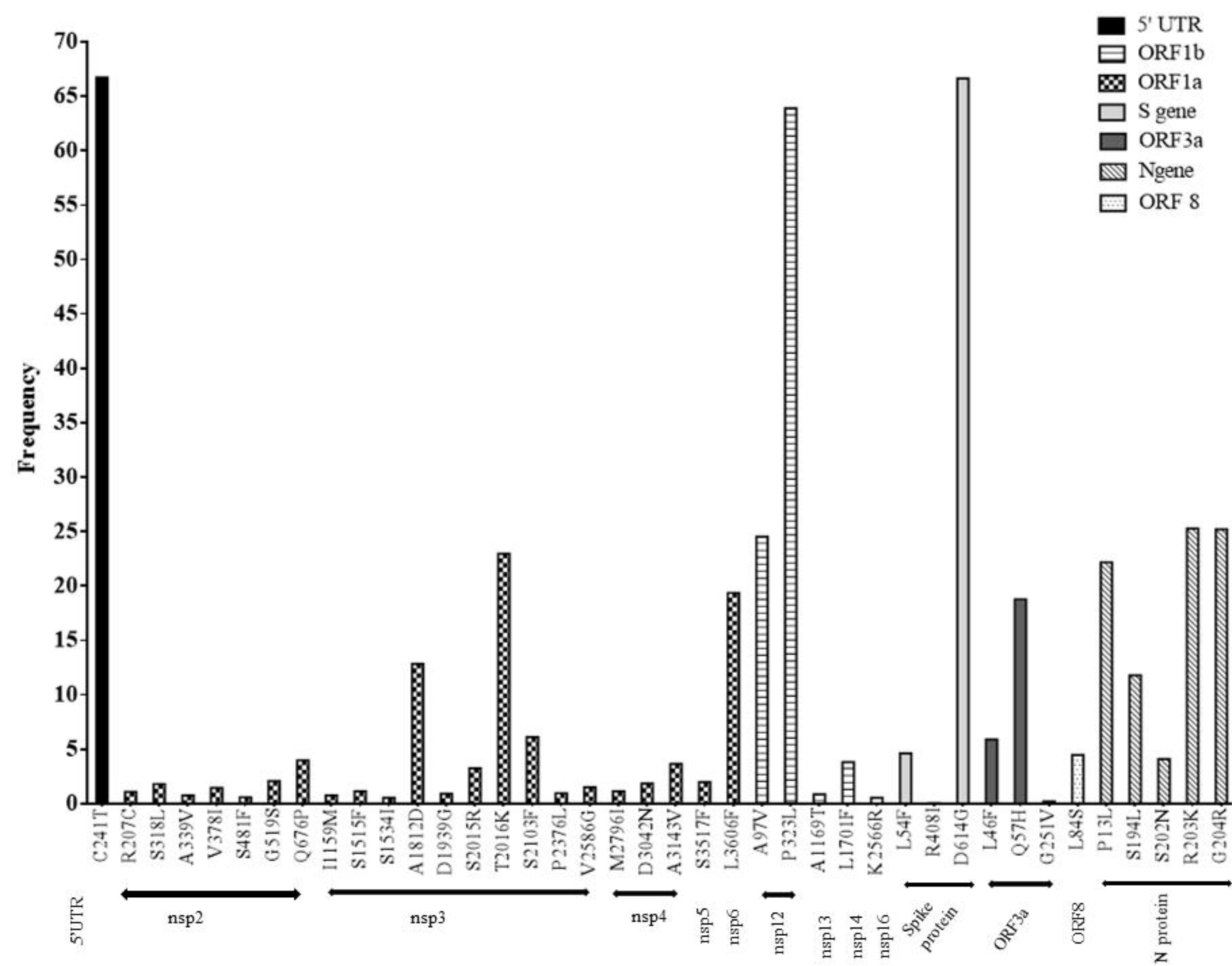


Fig 2: Distribution of non-synonymous mutations across the Indian SARS-CoV-2 genomes. Highest accumulation of mutations can be observed in ORF1a compared to the overall genome. Among the non-structural proteins, NSP3 tends to accumulate the greatest number of mutations..

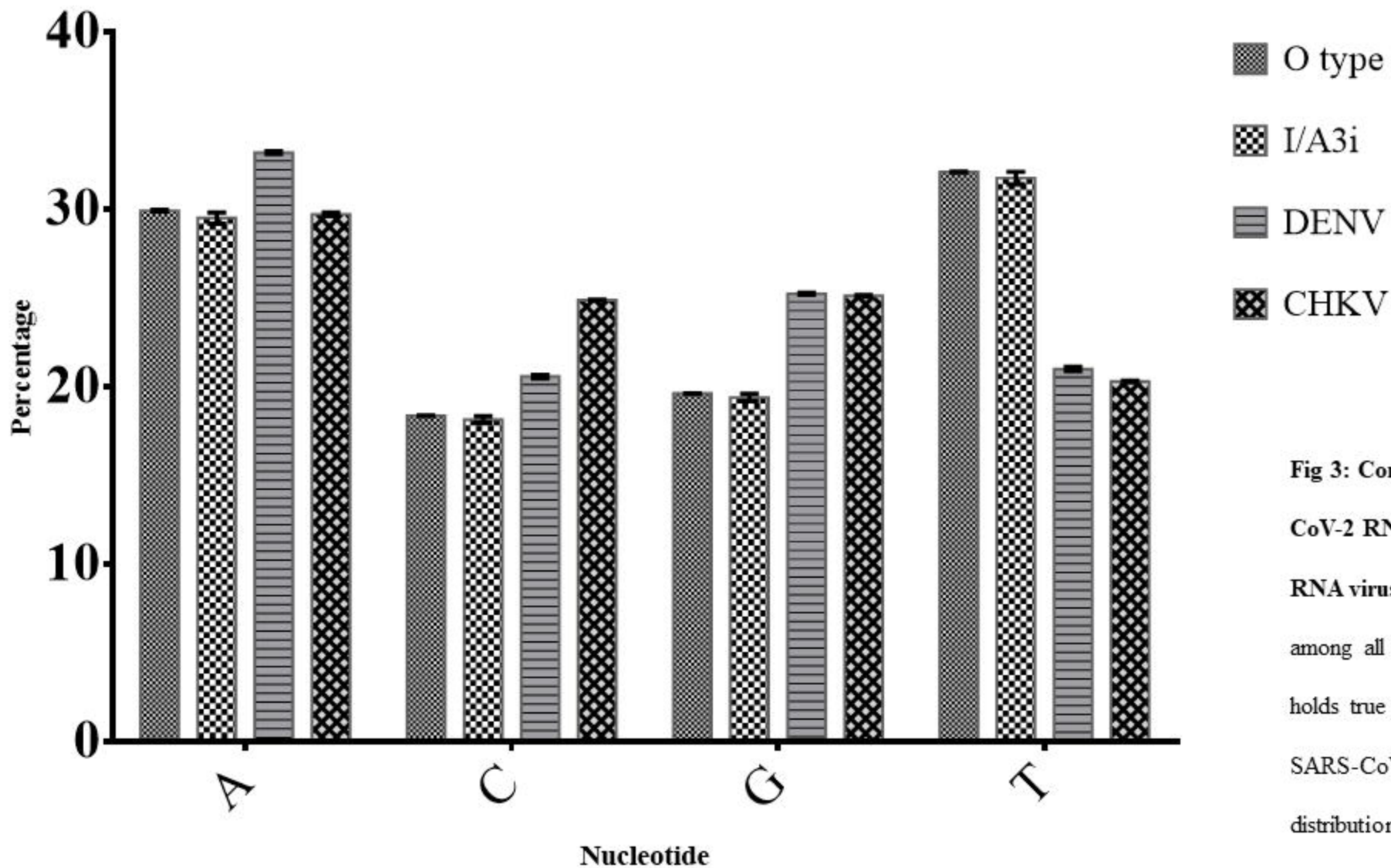


Fig 3: Comparison of nucleotide composition of SARS-CoV-2 RNA backbone with that of two other prevalent RNA viruses in India. The frequency of uracil is highest among all four nucleotides in SARS-CoV-2 genomes. This holds true for both older and recently emergent types of SARS-CoV-2 Indian sequences. Average nucleotide distribution in the RNA backbone of each virus was calculated from three sequences for each virus. Error bars represent SD among the three sequences of each virus used in the comparison.

Nucleotide changes frequency

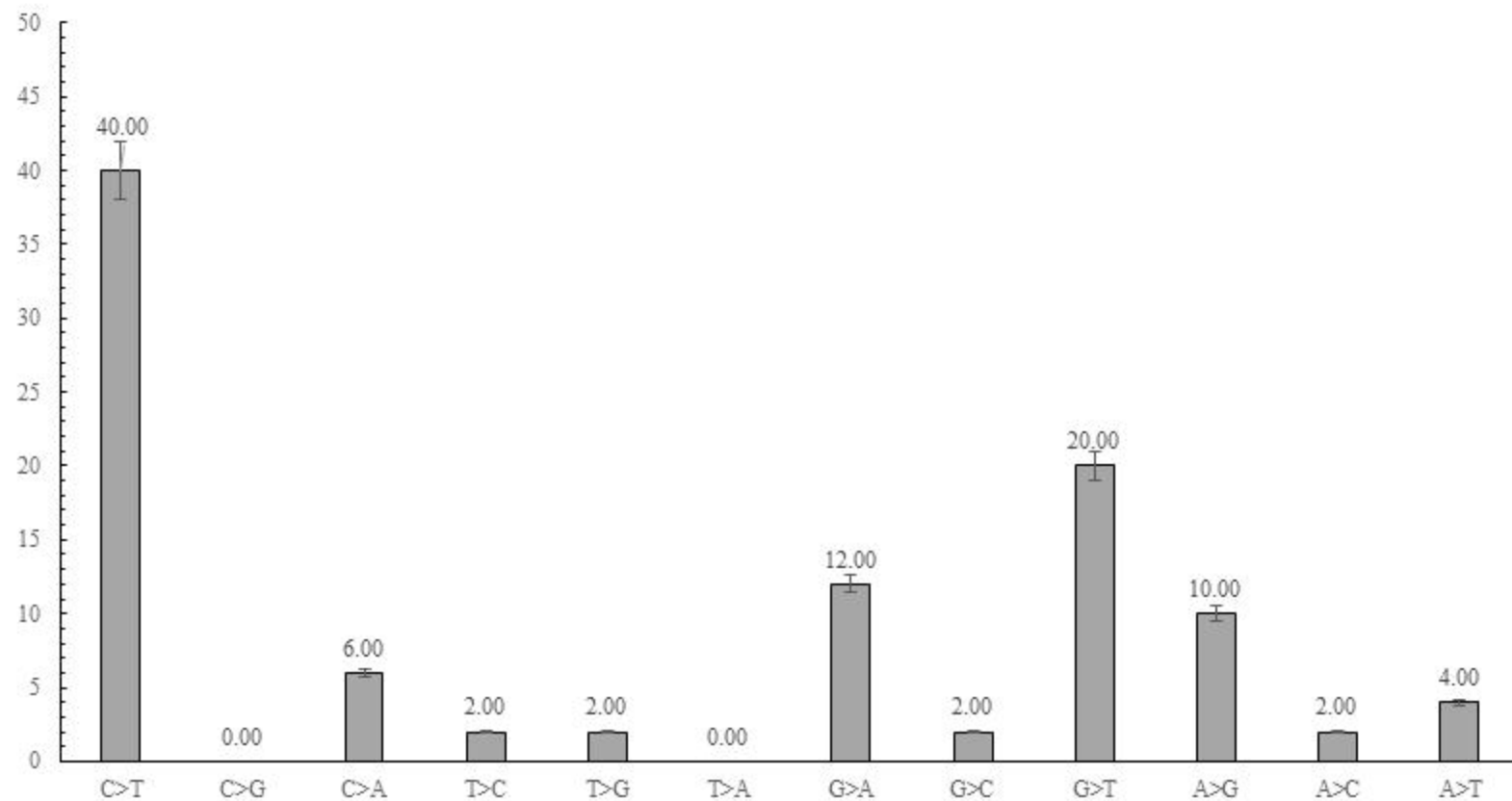


Fig 4: Frequency of non-synonymous nucleotide substitutions expressed as a percentage of the mutations resulting in amino acid substitutions. Most frequent changes in nucleotides were observed in form of C>T (40%). Substitution of G to T was recorded second-highest, sharing 20% of the total non-synonymous mutations. Overall, 64% of all the non-synonymous mutations were substitutions to uracil/thymidine.

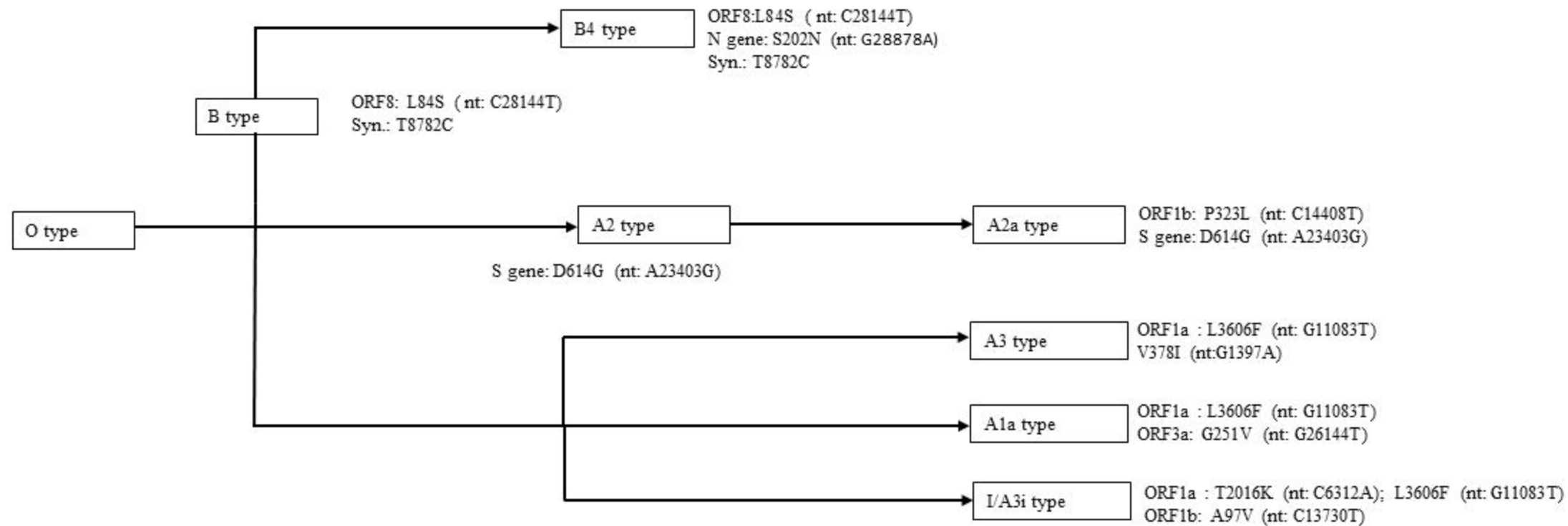


Fig 5: Schematic representation of SARS-CoV-2 types prevalent in the Indian population up to July 2020. It is based on the simplified understanding of the non-synonymous changes that shaped the emergence, divergence and prevalence of the different SARS-CoV-2 types.